MOLECULAR AND CELLULAR BIOLOGY, June 1991, p. 3191–3202
0270-7306/91/063191-12$02.00/0

Vol. 11, No. 6

The Juxtamembrane Regions of the Epidermal Growth Factor Receptor and gp185^{erbB-2} Determine the Specificity of Signal Transduction

ORESTE SEGATTO,[1]† * FULVIO LONARDO,[1] DANIEL WEXLER,[1] FRANCESCA FAZIOLI,[1] JACALYN H. PIERCE,[1] DONALD P. BOTTARO,[1] MORRIS F. WHITE,[2] AND PIER PAOLO DI FIORE[1]

Laboratory of Molecular and Cellular Biology, National Cancer Institute, Bethesda, Maryland 20892,[1] and Research Division, Joslin Diabetes Center, Department of Medicine, Harvard Medical School, Boston, Massachusetts 02215[2]

Received 4 December 1990/Accepted 16 March 1991

The epidermal growth factor receptor (EGFR) and gp185^{erbB-2} are closely related tyrosine kinases. Despite extensive sequence and structural homology, these two receptors display quantitative and qualitative differences in their ability to couple with mitogenic signalling pathways. By using chimeric molecules between EGFR and *erbB-2*, we found that the determinants responsible for the specificity of mitogenic signal transduction are located in the amino-terminal half of the tyrosine kinase domain of either receptor. In the EGFR, mutational analysis within this subdomain revealed that deletion of residues 660 to 667 impaired receptor mitogenic activity without affecting its tyrosine kinase properties. This sequence is therefore likely to contribute to the specificity of substrate recognition by the EGFR kinase.

Many growth factors regulate cellular growth, metabolism, and differentiation through activation of receptors endowed with intrinsic tyrosine kinase activity (1, 37, 44, 45). These receptors possess an extracellular ligand-binding domain; a hydrophobic domain, which anchors the receptor to the plasma membrane; and an intracellular portion, containing the tyrosine kinase domain (TK), which shows good sequence identity among the members of this family (16, 37, 45). Recently, progress has been made on the elucidation of the mechanisms of coupling between tyrosine kinase receptors and effector pathways (20, 21, 24–27, 37–40). The emerging picture is one of increasing complexity and underscores diversities in the use of a repertoire of effector molecules by different growth factor receptors. For instance, the platelet-derived growth factor receptor (PDGFR) phosphorylates phospholipase C-γ (PLC-γ) (25, 39) and the p21^{ras} GTPase-activating protein (GAP) (20, 21, 26) on tyrosine residues; however, other tyrosine kinase receptors do not (12, 26). Therefore, it appears that in addition to receptor expression and/or ligand availability, the specificity of substrate recognition contributes to determine the cellular response to a peptide growth factor.

The mechanisms involved in the transduction of the mitogenic signal by the epidermal growth factor (EGF) receptor (EGFR) (36) and the product of the *erbB-2* gene, gp185^{erbB-2} (5), appear to differ. In fact, even though closely related (5), EGFR and gp185^{erbB-2} show qualitative and quantitative differences in their ability to activate mitogenic pathways in different target cells under comparable conditions of expression and enzymatic activation. In NIH 3T3 fibroblasts, gp185^{erbB-2} displays a 100-fold higher transforming activity than the EGFR (8, 11). However, when expressed in 32D cells, an interleukin-3-dependent myeloid precursor cell line, the enzymatically active *erbB-2* product is unable to induce cell proliferation (11), whereas expression of the EGFR in this cell line induces EGF-dependent proliferation (30).

Since the intracellular domains of gp185^{erbB-2} and EGFR are only 15% homologous in their most COOH-terminal 250 residues, this region could confer differential coupling with postreceptor effector pathways (5). However, the COOH termini of EGFR and gp185^{erbB-2} appear to modulate intrinsic catalytic properties rather than specificity of substrate recognition (2, 10, 11, 33, 41). Specificity for coupling with postreceptor effector pathways was shown to reside instead in the highly conserved TK domains (11). In this study, we define the amino-terminal halves of their TK domains as the regions responsible for the specific coupling of the EGFR and gp185^{erbB-2} with their mitogenic pathways. A further mutational analysis of this subdomain led us to the identification of a region spanning residues 660 to 667 whose deletion markedly reduced EGFR mitogenic activity without affecting its intrinsic catalytic properties. This sequence might therefore be involved in the specific coupling of the EGFR with its effector pathways.

MATERIALS AND METHODS

Rationale and strategy of sequence comparison. The sequences of the TK domains of four pairs of the most closely related human growth factor receptors, i.e., EGFR and *erbB-2*, the insulin receptor (IR) and insulinlike growth factor-1 receptor (IGF-1R), c-*kit* and colony-stimulating factor type 1 receptor (CSF-1R), and PDGFR type α (PDGFR-α) and type β (PDGFR-β) (reviewed in references 16 and 45), were aligned. The end of the transmembrane region was assumed to be the NH_2-terminal boundary of the TK region. The COOH boundary was arbitrarily located at the Cys-Trp doublet (positions 926 and 927 in the EGFR sequence), which is absolutely conserved among receptor tyrosine kinases and after which no homology is easily detectable among these molecules. The sequence alignment was ini-

* Corresponding author.
† Present address: Department of Molecular Biology, Max-Planck Institute for Biochemistry, 8033 Martinsried bei Munchen, Federal Republic of Germany.

tially obtained with a GENALIGN program (Intelligenetics) and then modified visually to minimize the introduction of gaps. The homology score was assigned in a conservative fashion, and thus only a few of the accepted evolutionary conservative changes were scored as such, i.e., Asp for Glu and vice versa, Lys for Arg and vice versa, and any substitution among Ile, Leu, and Val (see legend to Fig. 1 for details).

Transfection and mitogenic assays. DNA transfection of NIH 3T3 (19) and NR6 cells (31) was performed by the calcium phosphate precipitation technique (15), as modified by Wigler et al. (43). Transformed foci were scored at 3 weeks. Where indicated, EGF (Upstate Biotechnology, 20 ng/ml) was added at day 14, and foci were scored at day 21. Transforming efficiency was calculated in focus-forming units (FFU) per picomole of added DNA after normalization for the efficiency of colony formation in parallel dishes subjected to selection in mycophenolic acid-containing medium (28). Cells expressing the *Ecogpt* gene were selected for their ability to form colonies in the presence of a mycophenolic acid-containing medium (28). [^{3}H]thymidine incorporation assays and the growth assay in chemically defined medium were performed as described previously (8, 14).

Engineering of eukaryotic expression vectors. The LTR-erbB-2 (9) and LTR-EGFR (8) expression vectors have been described previously. The chimeric expression vectors used in this study were engineered starting from LTR-erbB-2 and LTR-EGFR. Initially, novel *Sal*I and *Spe*I sites were engineered in identical positions in the sequences of *erbB-2* and EGFR bordering the TK1 region (see legend to Fig. 1 for a definition of TK1 and TK2), by site-directed mutagenesis (22) (see also Fig. 2 for graphic details). The *Sal*I sites were generated by modifying the sequences GGAGGC (nucleotides 2225 to 2230) and GGAGAC (nucleotides 2213 to 2218) of the EGFR (36) and *erbB-2* (5) open reading frames, respectively, to GTCGAC. The *Spe*I sites were similarly generated by modifying to ACTAGT the sequences CTT GGT and GCTCGT (nucleotides 2682 to 2687 and 2669 to 2674 for EGFR and *erbB-2*, respectively). These modifications did not alter the predicted protein sequences of EGFR and *erbB-2*. The 0.45-kbp *Sal*I-*Spe*I fragments encompassing the TK1 regions were then reciprocally swapped between EGFR and *erbB-2* to yield the LTR-erbB-2/EGFR^{TK1} and LTR-EGFR/erbB-2^{TK1} expression vectors. The amino acid boundaries of the TK1 regions were from positions 689 to 840 (numbered according to Coussens et al. [5]) and from positions 657 to 808 (numbered according to Ullrich et al. [36]) for *erbB-2* and EGFR, respectively. All of the constructions described were sequenced in both strands of the regions which underwent genetic manipulation.

Generation of EGFR mutants. EGFR mutants in the TK1 domain were generated in a 3-kbp *Sma*I-*Xho*I fragment of the EGFR cDNA (36) subcloned in M13mp19. Mutagenesis was performed according to Kunkel (22) with synthetic oligonucleotides. The positions of the amino acid deletions and substitutions (numbered according to the sequence by Ullrich et al. [36]) are indicated in Table 1. Substitutions were as follows: 1, Glu-Arg → Asp-Val; 5, Ser-Gly-Glu → Met-Val-Asn; 6, Lys → Asp; 9, Ser-Val-Asp-Asn → Leu-Glu-Leu-Arg; 10, Asp-Asn-Pro-His-Val → Leu-Ile-Pro-Glu-Phe; 12, Asp-Tyr-Val → Glu-Phe-Met; 14, His-Ile-Val → Val-Asn-Ser; 15, Gly-Ala → Thr-Met; 16, Ala-Glu-Glu-Lys → Val-Leu-Asp-Val. All the mutations were confirmed by DNA sequence analysis, and the mutants were subcloned into the LTR-2/EGFR expression vector (8).

TABLE 1. Enzymatic and biological properties of EGFR mutants[a]

Mutant no.	Type of mutation	Mutated residue(s)	Tyrosine kinase activity	Biological activity
1	Substitution	661–662	+	+
2	Deletion	660–667	+	+/−
4	Deletion	670–674	−	−
5	Substitution	671–673	−	−
6	Substitution	713	+	+
8	Deletion	742–750	−	−
9	Substitution	744–747	−	−
10	Substitution	746–750	−	−
11	Deletion	775–790	−	−
12	Substitution	776–778	+	+
14	Substitution	648–650	+	+
15	Substitution	839–840	+	+
16	Substitution	840–843	+/−	−

[a] Mutants are numbered here according to the code used in the original experimental protocols. Substitutions are detailed in Materials and Methods. Mutant cDNAs were subcloned in the LTR-EGFR expression vector (8) and transfected in NR6 fibroblasts. The biological activity of the transfectants was assessed as their ability to incorporate [^{3}H]thymidine upon EGF stimulation in comparison to wild-type EGFR transfectants derived in the same experiment. Tyrosine kinase activity was assayed as the ability of the mutant receptors to undergo in vivo autophosphorylation upon EGF triggering, as assessed by Western blot analysis of cell lysates with anti-PTyr antibodies. Symbols: +, activity comparable to wild-type EGFR; +/−, activity impaired compared with wild-type EGFR; −, absent or markedly diminished activity compared with wild-type EGFR.

Protein analysis. Total cellular proteins were obtained from mass cell populations derived after transfection and marker selection. Where indicated, cell lysis was performed after incubating cells at 37°C with EGF. Lysates were obtained in a buffer containing 50 mM HEPES (*N*-2-hydroxyethylpiperazine-*N'*-2-ethanesulfonic acid, pH 7.5), 150 mM NaCl, 1% Triton, 10% glycerol, 5 mM EGTA (ethylene glycol tetraacetic acid), phosphatase inhibitors (10 mM sodium pp$_i$ and 400 μM sodium orthovanadate), and protease inhibitors (1 mM phenylmethylsulfonyl fluoride and 10 μg of aprotinin per ml). Immunoprecipitation and immunoblot analyses were performed as described previously (10, 14, 33). Immunodetection was carried out with the M6 serum, directed against the *erbB-2* peptide 1218 to 1231 (10); the E7 serum, directed against the EGFR peptide 1172 to 1186 (10); a mixture of six monoclonal antibodies directed against PLC-γ (35); and an antiphosphotyrosine (anti-PTyr) affinity-purified polyclonal serum, prepared as described by Pang et al. (29). The specificity of immunodetection for the peptide antisera was controlled by performing parallel staining of identical blots with antibodies preabsorbed with the specific peptides (2 mg/ml). In the case of the anti-PTyr antibody, specificity was controlled by preabsorption of the antibody with either PTyr, phosphoserine, or phosphothreonine. In some cases a commercial anti-PTyr monoclonal antibody (UBI) was substituted for the anti-PTyr polyclonal serum, with comparable results.

In vitro kinase assays. Cell extracts were prepared from confluent monolayers incubated for 12 h in serum-free medium. Cell lysates were prepared in lysis buffer, containing 20 mM HEPES (pH 7.5), 150 mM NaCl, 10% glycerol, 1% Triton X-100, 1.5 mM MgCl, 1 mM phenylmethylsulfonyl fluoride, aprotinin (10 μg/ml), and leupeptin (10 μg/ml). Samples were normalized for amount of receptor by immunoprecipitation with a monoclonal antibody against the EGFR extracellular domain (Ab-1; Oncogene Science) followed by immunoblotting with EGFR antipeptide serum E7.

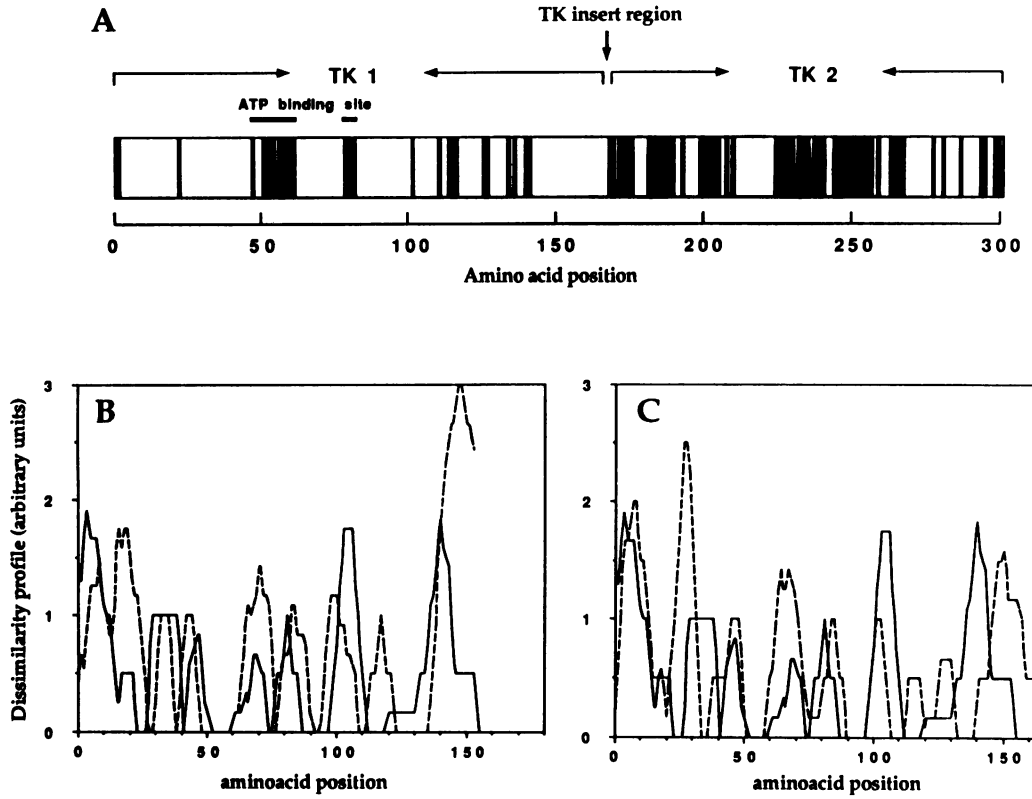

FIG. 1. Identification of two subdomains, TK1 and TK2, within the tyrosine kinase region of growth factor receptors. (A) Amino acid identity among tyrosine kinase growth factor receptors in their TK regions. The sequences of EGFR, *erbB-2*, IR, IGF-1R, CSF-1R, c-*kit*, PDGFR-α, and PDGFR-β were aligned as described in Materials and Methods. The figure depicts an ideal receptor tyrosine kinase (TK) region in which identities among the eight receptors are indicated with black bars and nonidentities are shown as blank spaces. Changes from Asp to Glu, Arg to Lys, and Ile to Leu or Val and vice versa were scored as identities. The insert TK region of CSF-1R, c-*kit*, PDGFR-α, and PDGFR-β is not shown in the diagram, but its approximate location is indicated by an arrow. The two horizontal black bars indicate residues involved in the creation of the ATP-binding site. Position 0 indicates the last amino acid in the transmembrane region of the analyzed receptors. (B and C) Dissimilarity profile in the TK1 region of pairs of closely related tyrosine kinase growth factor receptors. Individual pairs of closely related growth factor receptors (EGFR and *erbB-2*, IR and IGF-1R, and CSF-1R and c-*kit*) were analyzed for patterns of dissimilarity in the TK1 region. To obtain the dissimilarity profile of EGFR versus *erbB-2*, the amino acid sequences of their TK1 regions were aligned as described in Materials and Methods and then a preliminary arbitrary score was assigned to each single amino acid position in the alignment. Scores were 0 for identity of amino acid residues at any given position, 1 for conservative changes (Asp to Glu, Arg to Lys, and Ile to Val or Leu and vice versa), and 3 for nonconservative changes. The final dissimilarity scores were assigned at each single position by using an algorithm which arithmetically averaged the preliminary score of every residue with the scores of the residue immediately preceding and following it (window size, 6; value weights, 1 for each residue from position −3 to +3). The dissimilarity scores of IR versus IGF-1R and c-*kit* versus CSF-1R were obtained similarly. Panel B depicts the dissimilarity profile of the EGFR/*erbB-2* pair (solid line) matched to that for the c-*kit*/c-*fms* pair (dashed line). Panel C depicts the profile of the EGFR/*erbB-2* pair (solid line) matched to the dissimilarity profile of the IR/IGF-1R pair (dashed line).

For the in vitro autophosphorylation assay, lysates containing equal amounts of receptor were immunoprecipitated with the Ab-1 antibody, and the specific immunoprecipitates, recovered with protein G-agarose, were resuspended in 30 μl of HNTG (0.1% Triton X-100, 20 mM HEPES [pH 7.5], 150 mM NaCl, 10% glycerol) supplemented with 15 mM $MgCl_2$, 15 mM $MnCl_2$, 20 μCi of [γ-^{32}P]ATP (3,000 Ci/mmol; Amersham), and various concentrations of unlabeled ATP (final ATP concentration, 0.5 to 15 μM). Kinase reactions were performed for 1 min at 4°C (initial conditions) with shaking and were terminated by addition of 1 ml of washing buffer (35 mM EDTA and 1% Triton X-100 in HNTG). After centrifuging, each pellet was resuspended in 30 μl of sodium dodecyl sulfate (SDS) sample buffer and heated at 95°C for 5 min. This was repeated with an additional 50 μl of sample buffer, and the supernatants were pooled. ^{32}P incorporation into EGFR was measured by precipitation with trichloroacetic acid. Alternatively, the products of the kinase reaction were analyzed by 7.5% SDS–polyacrylamide gel electrophoresis (PAGE), and ^{32}P incorporation was measured by excising the receptor bands and scintillation counting after solubilization in Protosol tissue solubilizer (New England Nuclear). Both methods yielded comparable results.

The synthetic peptide KGSTAENAEYLRV, containing the Y1173 autophosphorylation site of the EGFR (13), was used as an in vitro substrate of the EGFR kinase. Conditions were as described for the autophosphorylation reaction; each reaction mix contained 20 μCi of [γ-^{32}P]ATP and, in addition, either 1 mM peptide and various concentrations of unlabeled ATP (for determining K_m ATP) or 0.0033 mM to 1 mM peptide in the presence of 15 μM ATP (for determining the K_m for peptide substrate). Reactions were terminated by adding 8 μl of 5× SDS sample buffer and heating at 95°C for 5 min. After centrifuging, the supernatants were analyzed by

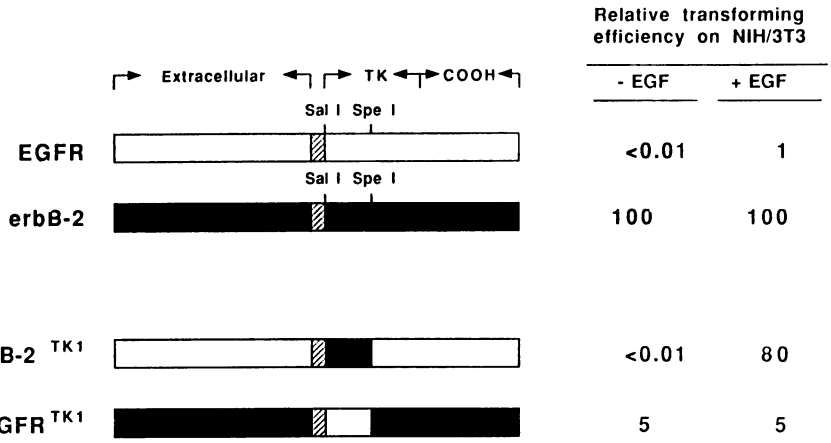

FIG. 2. Structure and biological activity of TK1 chimeric molecules between EGFR and *erbB-2*, expressed in NIH 3T3 cells. TK1 chimeric molecules were generated by reciprocally switching between the EGFR and *erbB-2* cDNA sequences encoding a stretch of 151 amino acids (residues 657 to 808 for EGFR and 689 to 840 for *erbB-2*) encompassed in the *SalI-SpeI* fragments, as discussed in Materials and Methods. The indicated expression vectors were transfected into NIH 3T3 cells by the calcium phosphate method as described before (15, 43), at 10-fold serial dilutions of plasmid DNA. Assays were scored at 3 weeks. Where indicated, EGF (20 ng/ml) was added at day 14 and assays were scored 1 week later. Focus-forming efficiency was calculated in FFU per picomole of added DNA as indicated in Materials and Methods. Results are expressed relative to the focus-forming activity (assigned a value of 1) of the wild-type LTR-EGFR plasmid (8) in cultures supplemented with EGF. In this latter condition, the LTR-EGFR expression vector induced transformation with an efficiency of about 1.0×10^2 to 2.0×10^2 FFU/pmol of DNA, compared with about 10^4 mycophenolic acid-resistant colonies per pmol of DNA (8–11). Data represent the average of at least three independent experiments performed in duplicate.

SDS-PAGE with a 20% acrylamide separation gel overlaid with a 7.5% gel. After autoradiography, the peptide bands were excised and counted as described above. Under our conditions of analysis, no significant difference was observed in the in vitro kinase assays performed in the absence of EGF or after treating the cell lysates with EGF (50 nM) at 22°C for 10 min prior to immunoprecipitation.

Phosphopeptide mapping. Tryptic peptide maps of EGFR were derived after immunoprecipitation and receptor auto-

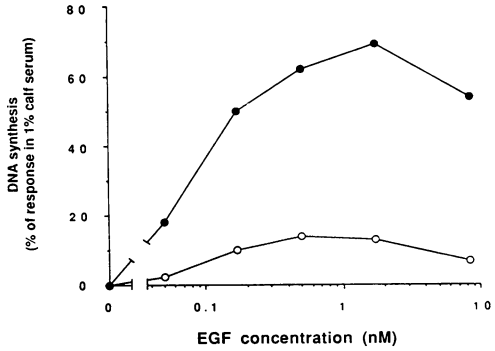

FIG. 3. Dose-response analysis of [^{3}H]thymidine incorporation upon EGF stimulation of quiescent NIH 3T3 fibroblasts expressing either wild-type EGFR or the EGFR/erbB-2 TK1 chimera. Cell lines were derived after transfection and marker selection; receptor number was assessed by [^{125}I]EGF binding; the NIH-EGFR and NIH-EGFR/erbB-2 TK1 cells used in these experiments expressed 2.7×10^5 and 2.5×10^5 receptors per cell, respectively. Cells were serum-starved for 60 h and then stimulated for 22 h with either 1% calf serum or the indicated concentration of EGF, in the presence of 4 μCi of [*methyl*-^{3}H]thymidine per well. Data from triplicate wells are expressed as the ratio [(EGF cpm − background cpm)/(1% serum cpm − background cpm)] × 100. Open circles, NIH-EGFR; solid circles, NIH-EGFR/erbB-2 TK1. Results are typical and representative of three independent experiments.

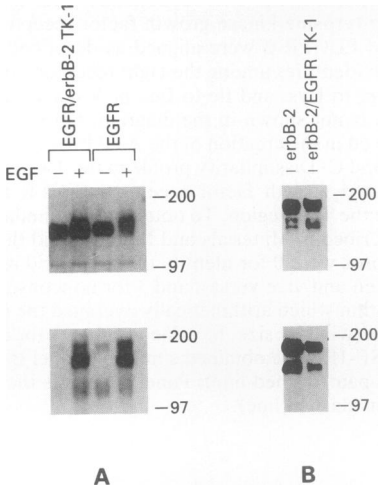

FIG. 4. Levels of expression and autophosphorylation activity in NIH 3T3 cells transfected with EGFR/erbB-2 TK1 and erbB-2/EGFR TK1 chimeras in comparison to their parental molecules. Lysates were prepared for serum-starved marker-selected mass populations of NIH 3T3 transfectants. Where indicated, cells were incubated with 16 nM EGF for 5 min at 37°C prior to lysis. Total cellular proteins (100 μg) were subjected to SDS-PAGE and blotted onto Immobilon membranes. Upper panels were probed either with the EGFR-specific antiserum E7 (left) or with the *erbB-2*-specific antiserum M6 (right). Lower panels were probed with anti-PTyr antibodies. (A) NIH-EGFR and NIH-EGFR/erbB-2 TK1 cells; (B) NIH-erb-2 and NIH-erbB-2/EGFR TK1 transfectants. In the case of *erbB-2* and erbB-2/EGFR TK1, tyrosine phosphorylation was observed in the absence of any added growth factors, whereas in the case of EGFR and EGFR/erbB-2 TK1, it was observed only upon EGF stimulation, in agreement with previous observations (10, 11). Results are typical and representative of three independent experiments. Molecular mass markers are indicated in kilodaltons.

phosphorylation in the presence of 50 μCi of [γ-^{32}P]ATP for 20 min at room temperature. Labeled immunoprecipitates were subjected to SDS-PAGE, receptor bands were excised, and SDS was removed by incubation with 20% methanol for 16 h at 37°C. The gel slices were then lyophilized, resuspended in 0.5 ml of 50 mM NH_4HCO_3 (pH 8.0), containing 200 μg of tolylsulfonyl phenylalanyl chloromethyl ketone (TPCK)-trypsin per ml, and incubated overnight at 37°C. The peptide-containing supernatant was lyophilized and dissolved in 0.05% trifluoroacetic acid, followed by C18 reversed-phase high-pressure liquid chromatography (HPLC). The column was eluted with a 0 to 75% acetonitrile gradient in 0.05% trifluoroacetic acid with a flow rate of 1.1 ml/min. Phosphopeptides eluting from the column were detected by Cerenkov counts with an on-line radiation detector (Radiomatic model A1-20). Samples of the peak fractions (one-fifth of the total) were also counted by scintillation.

EGF binding assay. For Scatchard analysis, 10^5 cells per well were seeded in 24-well tissue culture plates (Costar). The day after, culture medium was replaced with binding medium (Dulbecco's modified Eagle's medium containing 25 mM HEPES [pH 7.5] and 0.2% bovine serum albumin). After 2 h of incubation at 37°C, cells were shifted to 4°C and incubated with ^{125}I-EGF over a range of concentrations from 0.016 to 16 nM for at least 6 h. Assays were performed in triplicate wells, and specificity of binding was determined by parallel experiments in which a 100-fold molar excess of unlabeled EGF was used to compete with the tracer. To measure downregulation of high-affinity EGF-binding sites by phorbol esters, cells were incubated for 1 h with 100 nM phorbol myristate acetate (PMA; Sigma) at 37°C before performing the binding assay. Conditions were the same as above, except that binding was measured in the presence of 100 nM PMA. After incubation with EGF, cells were washed six times with ice-cold binding medium and solubilized with 10 mM NaOH–1% SDS. Radioactivity was measured in a Beckman gamma counter. The number of receptors per cell and their dissociation constant (K_d) for EGF were determined from Scatchard plots. Analysis of the binding was performed with the LIGAND software.

RESULTS

Sequence divergence in the kinase domain of EGFR and gp185^{erbB-2}. Alignment of the predicted primary sequence of the catalytic domains of EGFR and gp185^{erbB-2} shows an overall amino acid sequence identity of about 80% (5), with most of the differences clustered in a few discrete areas. Based on the pattern of conservation among receptors from different subfamilies, however, this domain can be divided into two subdomains, TK1 and TK2 (Fig. 1A). The TK2 domain shows the least sequence variability, which suggests that it might form the structural core for the phosphotransferase reaction (Fig. 1A) (16). The TK1 subdomain, on the other hand, is poorly conserved among the various receptor subfamilies (Fig. 1A) (16), although it retains a high degree of similarity among receptors of the same subfamily.

We searched for profiles of sequence divergence in the TK1 domain of different pairs of closely related receptors. We chose three pairs of receptors (see legend to Fig. 1 for details), the members of each pair having evolved from a similarly distant branching point of the evolutionary tree of tyrosine kinases (16). The computer analysis shown in Fig. 1B and 1C indicates that among different pairs of receptors, the clusters of sequence divergence in their TK1 domains fall into similar positions, which suggests that evolutionary pressure favored variability of a limited number of sequences in the TK1 domain of tyrosine kinase receptors.

The NH_2-terminal half of the EGFR and *erbB-2* kinase domain determines specificity of signal transduction. If sequence variability in the TK1 domain were responsible for specificity of coupling with mitogenic pathways, then exchanging the TK1 domains between gp185^{erbB-2} and EGFR should confer *erbB-2*-like properties on the latter and vice versa. We engineered such chimeric molecules, designated EGFR/erbB-2 TK1 and erbB-2/EGFR TK1, and transfected them into NIH 3T3 fibroblasts. As previously shown (8–11), the parental *erbB-2* expression vector induced transformation at least 100-fold more efficiently than EGFR, even when the latter was maximally stimulated by EGF addition (Fig. 2). Switching the *erbB-2* TK1 domain into EGFR markedly increased the EGFR transforming efficiency, which was still dependent on EGF supplementation (Fig. 2). Conversely, the erb-2/EGFR TK1 construct displayed greatly reduced focus-forming activity compared with the *erbB-2* molecule. Therefore, the transforming activity of the chimeras segregated with that of the wild-type cDNAs from which the TK1 domains were derived.

We took advantage of the ligand dependence of EGFR signalling to compare the mitogenic response to EGF of NIH 3T3 cells transfected with wild-type EGFR and EGFR/erbB-2 TK1 molecules. As shown in Fig. 3, at comparable levels of receptor expression, the NIH-EGFR/erbB-2 TK1 cells showed a four- to fivefold-higher mitogenic response to EGF than NIH-EGFR cells; however, the 50% effective dose (ED_{50}) for EGF was comparable for both cell lines (about 0.1 nM EGF). The difference between these two cell lines in the magnitude of their maximal mitogenic response to EGF, despite similar ED_{50} values, affinity for EGF binding (data not shown), and receptor levels (see also below), is compatible with the concept that the EGFR and *erbB-2* effector pathways are qualitatively different and that specificity of substrate recognition is conferred by their TK1 domains.

Western immunoblot analysis of mass populations of NIH 3T3 transfectants derived after marker selection showed that the levels of expression of wild-type and chimeric receptors were comparable (Fig. 4). Furthermore, no difference in the level of tyrosine phosphorylation in vivo was detected between gp185^{erbB-2} and the erbB-2/EGFR TK1 chimeras or between the EGFR and the EGFR/erbB-2 TK1 chimeras (Fig. 4) under appropriate conditions of stimulation. It has been shown previously that the level of tyrosine phosphorylation in vivo correlates well with gp185^{erbB-2} and EGFR kinase activity (10, 32–34). Thus, since differences in neither receptor expression nor kinase activity in vivo could account for the observed biological differences, we conclude that structural determinants located in the TK1 subdomain of the EGFR and the *erbB-2* product must be responsible for their specific coupling with different mitogenic pathways.

Mutational analysis of the TK1 domain of the EGFR. As discussed above, the sequences of the EGFR and gp185^{erbB-2} in their TK1 regions differ in only a few discrete areas. Then, in principle, mutations targeted to these regions might be sufficient to impair mitogenic signalling without affecting the phosphotransferase activity of the receptor. We chose to use the EGFR to pursue this experimental approach, since the availability of a ligand allows precise quantitative measurements of biological activity and receptor expression.

Mutations were introduced in the EGFR cDNA coding sequence in order to obtain either deletions or amino acid substitutions within the TK1 sequences which diverge from

erbB-2 (Table 1), and the mutants were transfected into NR6 fibroblasts, which are devoid of endogenous EGFR (31). The sequence containing EGFR residues 839 to 844, located in TK2, was also included as a target for mutations because of its high divergence between EGFR and gp185^{erbB-2}. Cell lines expressing individual mutants were obtained after marker selection and screened for mitogenic response and autophosphorylation in vivo upon EGF triggering. The results of the initial screening are summarized in Table 1. The mutants in which we could not detect EGF-dependent tyrosine autophosphorylation despite receptor expression (mutants 4, 5, 8, 9, 10, 11, and 16) were also unable to transduce a mitogenic signal (Table 1). These mutants were not investigated further, since the mutations were likely to have affected the intrinsic enzymatic activity of the receptor. Mutants 1, 2, 6, 12, 14, and 15 showed catalytic activity in vivo and were mitogenically active.

To obtain cell lines expressing similar levels of the latter mutants, NR6 transfectants were subjected to fluorescence-activated cell sorting (FACS) analysis with a monoclonal antibody against the extracellular domain of the human EGFR in an indirect immunofluorescence assay. ^{125}I-EGF binding confirmed that these cell lines expressed similar levels of receptors (data not shown). FACS-derived cell lines expressing EGFR mutants 1, 6, 12, 14, and 15 exhibited a mitogenic response to EGF which was indistinguishable from that of wild-type EGFR (Table 1) and were not analyzed further. However, cell lines expressing mutant 2 (referred to as EGFR Δ660-667 henceforth) were found to be mitogenically less responsive to EGF than cell lines expressing wild-type EGFR despite comparable levels of expression and autophosphorylation activity. This phenomenon was reproducibly observed with cells derived from two independent transfections and sorting experiments.

Figure 5A shows a typical EGF dose-response experiment for cell lines expressing about 2×10^4 receptors per cell of either wild-type EGFR or EGFR Δ660-667. The maximal response of the Δ660-667 mutant was about eightfold lower than that of the wild-type EGFR. At levels of expression of about 10^5 receptors per cell, the maximal response to EGF of the Δ660-667 mutant was 30 to 40% of that obtained with wild-type EGFR (Fig. 5B). In both experiments we also observed a three- to fivefold increase in the ED_{50} for EGF of cells expressing the Δ660-667 mutant. These results were paralleled by those obtained in a growth assay in chemically defined medium under conditions in which cell growth is strictly EGF dependent. While no difference was detected in the ability to grow in 1% serum, EGF-dependent growth was impaired in NR6-EGFR Δ660-667 compared with that in NR6-EGFR. NR6-EGFR Δ660-667 growth was reduced by about 30% in medium containing 1 nM EGF and by 50 to 60% in medium containing 0.15 nM EGF compared with that of NR6-EGFR expressing similar numbers of receptors (Table 2).

The Δ660-667 mutation does not alter EGFR affinity for EGF or its intrinsic catalytic properties. The above biological analysis indicated that the Δ660-667 mutation impairs the ability of the EGFR to transduce a mitogenic signal. While it was possible that the Δ660-667 mutation affects the ability of the EGFR to recognize cellular substrates important in the transduction of the mitogenic signal, differences in either the intrinsic kinase activity or the EGF-binding affinities of the Δ660-667 mutant may also account for the observed alterations of biological behavior.

To resolve these possibilities, we evaluated the EGF-binding properties of the Δ660-667 mutant and wild-type EGFR. As shown in Table 3, both NR6-EGFR and NR6-EGFR Δ660-667 expressed two classes of receptors having dissociation constants (K_ds) in the range of 10^{-9} M (low-affinity sites) and 10^{-10} M (high-affinity sites) (6). Treatment with phorbol esters led to the disappearance of high-affinity sites in NR6-EGFR, as published previously (6), as well as in NR6-EGFR Δ660-667 (Table 3). Therefore, the quantitative partition of high- versus low-affinity sites, the affinity constants, and the regulation of receptor affinity by phorbol esters were similar in NR6-EGFR Δ660-667 and NR6-EGFR (Table 3).

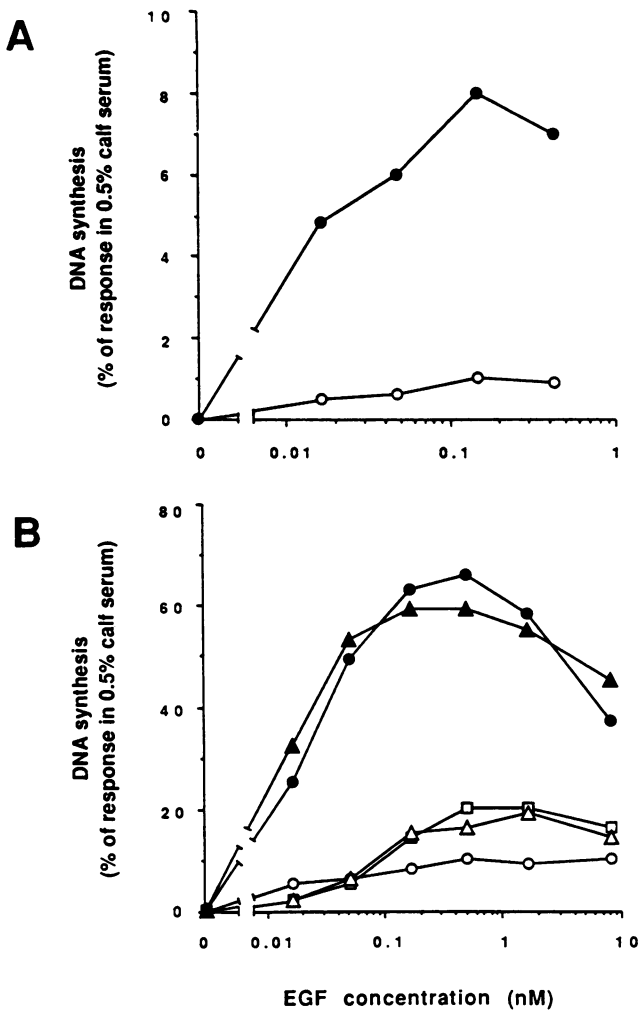

FIG. 5. Dose-response analysis of [^{3}H]thymidine incorporation upon EGF stimulation of quiescent NR6 fibroblasts expressing either EGFR Δ660-667 or wild-type EGFR. Cell lines obtained by two independent transfection and selection experiments were serum-starved for 60 h and then stimulated for 22 h either with 0.5% serum or with the indicated concentrations of EGF in the presence of 4 μCi of [*methyl*-^{3}H]thymidine per well. Data are expressed as the ratio [(EGF cpm − background cpm)/(0.5% serum cpm − background cpm)] × 100. Open symbols, NR6-EGFR Δ660-667; solid symbols, NR6-EGFR. (A) The number of ^{125}I-EGF-binding sites per cell was 1.8×10^4 and 1.9×10^4 for NR6-EGFR Δ660-667 and NR6-EGFR, respectively. Cell lines used for the experiment depicted in panel B expressed the following numbers of ^{125}I-EGF-binding sites: □, 7.1×10^4; ○, 6.5×10^4; △, 10×10^4; ■, 8.5×10^4; ▲, 11×10^4. Results are typical and representative of three experiments performed in triplicate.

TABLE 2. EGF-dependent cell growth of NR6-EGFR and NR6-EGFR Δ660-667 cells in chemically defined medium[a]

Expt no.	Avg no. of cells in medium with[b]:			
	I	I + E (1 nM)	I + E (0.15 nM)	1% CS
1				
EGFR wild type	30,000	156,200	96,200	251,900
EGFR Δ660-667	36,300	104,400	59,400	253,800
2				
EGFR wild type	34,000	165,400	140,400	358,000
EGFR Δ660-667	43,300	99,800	70,000	335,900
EGFR Δ660-667	31,300	84,500	53,600	362,000

[a] Cells (4×10^4) were plated on 60-mm dishes coated with poly-D-lysine. Cells were counted after 5 days. Numbers represent the average cell counts of duplicate dishes in two independent experiments. NR6 transfectants expressing about 10^5 receptors per cell were used in both experiments. In experiment 2, two independently derived NR6-EGFR Δ660-667 transfectants were used.
[b] I, insulin (5 μg/ml); E, EGF (1 or 0.15 nM); CS, calf serum.

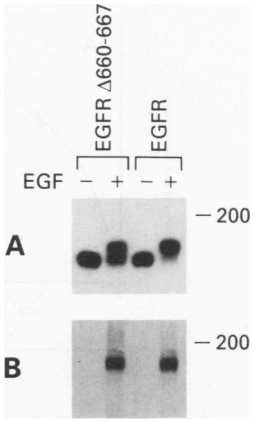

FIG. 6. EGF-dependent autophosphorylation in vivo of wild-type EGFR and EGFR Δ660-667. NR6 transfectants expressing either wild-type or mutant receptors were serum-starved for 6 h, incubated for 5 min at 37°C with 16 nM EGF or in serum-free medium, and lysed thereafter. One hundred micrograms of total cellular protein from each sample was subjected to SDS-PAGE and Western blot analysis. The upper panel was probed with the EGFR-specific E7 antiserum; the lower panel was probed with anti-PTyr antibodies. Results are representative of three experiments. Molecular mass markers are indicated in kilodaltons.

As discussed above, EGFR mutations in the TK1 region were initially screened for their ability to undergo EGF-dependent autophosphorylation in vivo. Figure 6 depicts an analysis in which Western blots of cell lysates obtained from NR6-EGFR and NR6-EGFR Δ660-667 cells were probed with either an anti-EGFR antiserum (Fig. 6A) or an anti-PTyr antibody (Fig. 6B). In this experiment, cells were incubated for 5 min at 37°C with 16 nM EGF prior to lysis, resulting in a comparable level of autophosphorylation of EGFR Δ660-667 and wild-type EGFR. Similar results were obtained when the incubation with EGF was shortened to 1 min, when a 10-fold-lower concentration of EGF was used (data not shown), when labeling with ^{32}P in vivo was followed by incubation with 16 nM EGF (1 or 5 min at 37°C), and when immunoprecipitation with anti-PTyr antibodies was done (data not shown). These results show that the EGFR Δ660-667 mutant is able to undergo EGF-dependent autophosphorylation in vivo with the same efficiency as wild-type EGFR.

We next performed a kinetic study of the catalytic properties of the wild-type EGFR and EGFR Δ660-667 mutant in vitro. For this purpose, we used an assay in which the ability of the immunoprecipitated receptor to undergo autophosphorylation in vitro could be correlated with its ability to phosphorylate a synthetic exogenous substrate on tyrosine residues. Cell lysates were prepared from NR6-EGFR and NR6-EGFR Δ660-667, and the receptor content in each lysate was estimated by immunoblot analysis of serial dilutions of the lysates. Quantitatively immunoprecipitated wild-type and mutant EGFR showed specific autophosphorylation activity that was independent of receptor concentration in the immunoprecipitate (data not shown). The initial rate (i.e., 1 min of incubation at 4°C) of autophosphorylation of wild-type EGFR and EGFR Δ660-667 showed a similar dependence on ATP concentration (Fig. 7A and B), with a K_m of 3 to 4 μM for both molecules. Likewise, the velocity of peptide substrate phosphorylation showed a similar profile of dependence on either ATP or peptide concentration for both the wild-type and mutant receptors, with a K_m of 4 to 5 μM for ATP (Fig. 7C and D) and 180 to 190 μM for the peptide (Fig. 7E and F). Furthermore, no differences could be observed in the HPLC profile of tryptic phosphopeptides obtained after in vitro autophosphorylation of either wild-type or Δ660-667 EGFR (Fig. 8), indicating that the sites of in vitro autophosphorylation of the Δ660-667 mutant were the same as those of wild-type EGFR. Taken together, these results demonstrate that the impaired signalling properties of the EGFR Δ660-667 mutant cannot be ascribed to either reduced affinity for EGF or alterations of its intrinsic tyrosine kinase activity.

TABLE 3. Analysis of the ^{125}I-EGF-binding properties of NR6-EGFR and NR6-EGFR Δ660-667 cells[a]

Receptor	High affinity		Low affinity	
	No. of receptors/cell	K_d (nM)	No. of receptors/cell	K_d (nM)
Wild-type EGFR	10,000	0.10	110,000	6.3
Wild-type EGFR + PMA			115,000	7.6
EGFR Δ660-667	9,000	0.07	128,000	4.4
EGFR Δ660-667 + PMA			141,000	4.8

[a] ^{125}I-EGF binding was assessed by Scatchard analysis over a range of concentrations from 0.016 to 16 nM in triplicate wells. Specificity of binding was controlled in a parallel competition experiment by using a 100-fold molar excess of unlabeled EGF. Where indicated, binding experiments were performed in the presence of 100 nM PMA. Data were analyzed with the LIGAND software.

PLC-γ phosphorylation by the EGFR Δ660-667 mutant in vivo. Recently, several groups have reported that the γ isozyme of phospholipase C (PLC-γ) is physically associated with and is a substrate of ligand-activated EGFR and PDGFR (24, 25, 39, 40). In an attempt to characterize the ability of the EGFR Δ660-667 mutant to recognize physiological EGFR substrates, we investigated its ability to phosphorylate PLC-γ on tyrosine residues. NR6-EGFR and NR6-EGFR Δ660-667 cells expressing a comparable level of receptors (Fig. 9C) were treated with EGF for 5 min at 37°C prior to lysis. Equal amounts of cellular proteins from either cell line were immunoprecipitated with excess anti-PTyr antibodies and then subjected to immunoblot analysis with a mixture of anti-PLC-γ monoclonal antibodies (35). No quantitative difference was observed in the EGF-dependent phosphorylation of PLC-γ on tyrosine residues in immunoprecip-

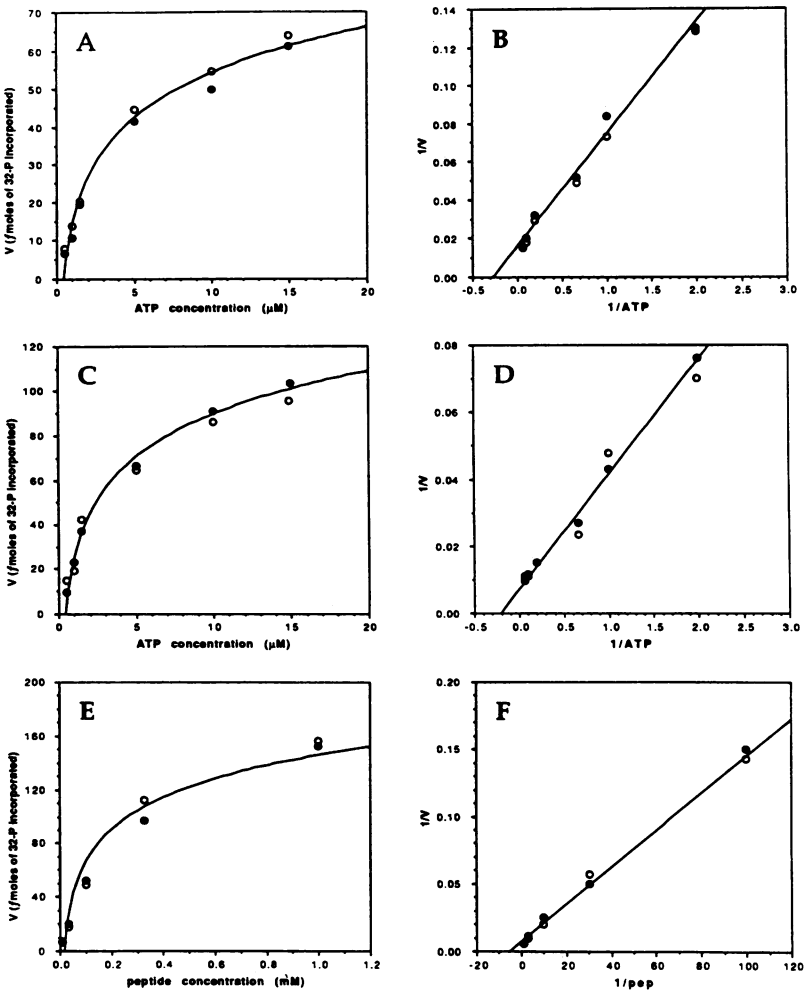

FIG. 7. Analysis of the catalytic properties of wild-type EGFR and EGFR Δ660-667 in vitro. Lysates were prepared from NR6 transfectants, and equal amounts of receptor were immunoprecipitated for in vitro assays. Reactions were carried out at the initial rate for 1 min at 4°C. In preliminary experiments, the specific autokinase activity of both EGFR and EGFR Δ660-667 was found to be independent of receptor concentration in the immunoprecipitates (not shown). Open circles, wild-type EGFR; solid circles, EGFR Δ660-667. (A and B) Receptor autophosphorylation activity was assayed as a function of ATP concentration. (C, D, E, F) Receptors were assayed for their ability to phosphorylate the synthetic peptide KGSTAENAEYLRV, containing the Y1173 autophosphorylation site of the EGFR. The velocity of peptide phosphorylation was assayed as a function of ATP concentration in panels C and D and as a function of peptide concentration in panels E and F. (A, C, E) Michaelis-Menten plots; (B, D, F) Lineweaver-Burk plots. Results are representative of three independent experiments performed in triplicate.

itates from both NR6-EGFR and NR6-EGFR Δ660-667 (Fig. 9A). Since neither the steady-state level of PLC-γ nor the level of receptors (Fig. 9B and C) was different in the two cell lines examined, we conclude that the Δ660-667 mutant was able to phosphorylate PLC-γ with the same efficiency as wild-type EGFR.

We next evaluated the ability of the wild-type and Δ660-667 EGFRs to couple with the phosphatidylinositol turnover pathway by measuring the formation of inositol phosphates in cells labeled with *myo*-[^{3}H]inositol. As shown in Table 4, activation of the EGFR kinase induced the formation of [^{3}H]inositol phosphates in NR6-EGFR cells. The ability of an active EGFR kinase to stimulate PIP_2 breakdown was, however, significantly lower than that of PDGFR expressed at comparable levels (Table 4), consistent with our previous observations (14). Moreover, no major difference in [^{3}H] inositol phosphate formation was observed in NR6-EGFR and NR6-EGFR Δ660-667 cells treated with EGF, consistent with their comparable efficiency of PLC-γ phosphorylation (Table 4).

Tyrosine phosphorylation of cellular proteins by EGFR and EGFR Δ660-667. We next analyzed the ability of EGFR and EGFR Δ660-667 to phosphorylate cellular proteins on tyrosine residues. To this end, NR6-EGFR and NR6-EGFR Δ660-667 cells expressing comparable levels of receptors (Fig. 9C) were metabolically labeled with $^{32}P_i$ and then treated with EGF or mock-treated prior to lysing. Cellular lysates were immunoprecipitated with an anti-PTyr antibody and analyzed by SDS-PAGE. As shown in Fig. 10A, treatment of NR6-EGFR and NR6-EGFR Δ660-667 with EGF for 1 or 5 min resulted in increased tyrosine phosphorylation of a number of cellular proteins. Major 170-kDa species corresponded to the EGFR and the EGFR Δ660-667 (Fig. 10A). Other proteins phosphorylated on tyrosine by active EGFRs included species of approximately >200, 115 (14), 95, 85, 72 to 75, 60, 52, and 45 kDa. None of these proteins displayed

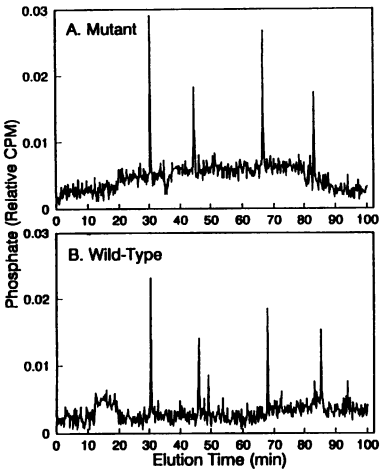

FIG. 8. Tryptic phosphopeptide maps of wild-type EGFR and EGFR Δ660-667 phosphorylated in vitro with [γ-^{32}P]ATP. Similar amounts of either wild-type (B) or mutant (A) EGFR were immunoprecipitated from NR6-EGFR or NR6-EGFR Δ660-667 cells. Immunoprecipitates were subjected to in vitro autophosphorylation with [γ-^{32}P]ATP and analyzed by SDS-PAGE. Receptor bands were then excised and subjected to extensive trypsin digestion. Peptides were separated by reversed-phase HPLC. Eluted phosphopeptides were detected by Cerenkov counts with an on-line radiation detector and are expressed as cpm relative to the entire input sample. Aliquots of the peak fractions (one-fifth of the total) were also analyzed by scintillation counting with the following results (peaks are numbered from left to right). Mutant: first peak, 1,148 cpm; second peak, 737 cpm; third peak, 859 cpm; fourth peak, 469 cpm. Wild-type: first peak, 722 cpm; second peak, 464 cpm; third peak, 516 cpm; fourth peak, 354 cpm.

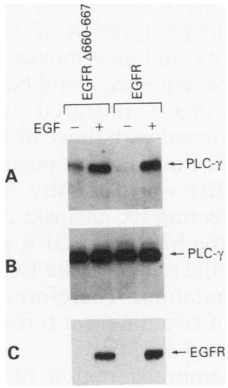

FIG. 9. Analysis of tyrosine phosphorylation of PLC-γ in NR6-EGFR and NR6-EGFR Δ660-667. Cells were serum-starved for 16 h and then stimulated for 5 min at 37°C with 16 nM EGF (EGF+) or mock treated (EGF−) and lysed thereafter. Four milligrams of total cellular proteins from each lysate was immunoprecipitated with excess anti-PTyr antibodies and immunoblotted with anti-PLC-γ monoclonal antibodies (A). A similar amount of PLC-γ was detectable in 100 μg of each lysate by performing immunoblot analysis with anti-PLC-γ antibodies before the immunoprecipitation (B). Cell lines used in this experiment expressed comparable levels of receptor, as shown by the amount of autophosphorylated EGFR detected by anti-PTyr antibodies in panel C (by ^{125}I-EGF-binding experiments, these cell lines were found to express about 1.0×10^5 EGFRs or EGFR Δ660-667s per cell, respectively). Results are typical and representative of four independent experiments.

TABLE 4. Effects of EGF and PDGF-BB on inositol phosphate formation in NR6, NR6-EGFR, and NR6-EGFR Δ660-667 cells[a]

Treatment	Fold stimulation (mean ± SE, n = 4)		
	NR6	NR6-EGFR	NR6-EGFR Δ660-667
No addition	1.00 ± 0.01	1.00 ± 0.01	1.00 ± 0.02
EGF	1.01 ± 0.03	1.54 ± 0.13	1.41 ± 0.06
PDGF	8.84 ± 0.57	10.86 ± 1.08	8.92 ± 0.91

[a] Subconfluent cultures of NR6, NR6-EGFR, and NR6-EGFR Δ660-667 cells were labeled with *myo*-[^{3}H]inositol and stimulated with the different agonists for 30 min as described previously (14). Inositol phosphates were analyzed by anion-exchange chromatography. Results were normalized for the value of total inositol-containing phospholipids and are expressed as fold stimulation over control (unstimulated) values for each cell line. Basal level of inositol phosphates in a representative experiment of NR6-EGFR cells was 7,999 ± 210 cpm (IP1, 5,305 ± 335; IP2, 2,559 ± 168; IP3, 135 ± 11). After stimulation with EGF for 30 min, the levels were: IP1, 9,373 ± 745; IP2, 2,479 ± 512; IP3, 196 ± 21; total, 12,050 ± 885 cpm. The preponderance of inositol monophosphates after 30 min of stimulation with EGF is due to the rapid dephosphorylation of calcium-mobilizing inositol phosphates which were formed during the initial phase of stimulation. The NR6-EGFR and NR6-EGFR Δ660-667 cells used in these experiments expressed about 1.0×10^5 EGFRs or EGFR Δ660-667s per cell, respectively, and both expressed about 1.0×10^5 to 1.5×10^5 PDGFRs per cell.

lower PTyr content in NR6-EGFR Δ660-667 than in NR6-EGFR cells under conditions of EGF stimulation.

As an alternative approach, we immunoprecipitated, with anti-PTyr antibodies, PTyr-containing proteins from NR6-EGFR and NR6-EGFR Δ660-667 cells treated with EGF in vivo and analyzed them by immunoblot with anti-PTyr antibodies. As shown in Fig. 10B, PTyr-containing proteins were identified by this approach which corresponded to those detected in ^{32}P-labeled lysates, namely species of ~170 (EGFR), 115, 72 to 75, 60, 52, and 45 kDa. Also in this case, however, no significant difference was detected in the pattern of PTyr-containing proteins in EGF-stimulated NR6-EGFR and NR6-EGFR Δ660-667 cells (Fig. 10B).

DISCUSSION

Previous studies have indicated that the tyrosine kinase domains of the EGFR and *erbB-2* products dictate specificity of mitogenic signal transduction (11). By sequence comparison of EGFR and *erbB-2* as well as of other pairs of closely related receptors, we found that the amino-terminal portion of their tyrosine kinase domains (TK1 region) had the greater degree of sequence divergence. This suggested that the TK1 might contain determinants which impart specificity of coupling with postreceptor effector pathways. Indeed, by switching the TK1 domain of *erbB-2* into the EGFR (EGFR/erbB-2 TK1 chimera), we could essentially confer to this chimera *erbB-2*-like mitogenic properties in fibroblasts. Conversely, the erbB-2/EGFR TK1 chimera showed a marked reduction in transforming activity in NIH 3T3 cells compared with the parental *erbB-2* product.

The qualitative nature of this phenomenon was further confirmed by gene transfer experiments performed in the 32D hematopoietic cell line. In line with our previous observations (11), the EGFR-like phenotype of the erbB-2/EGFR TK1 chimera in fibroblasts was mirrored by its ability to abrogate interleukin-3 dependence in 32D cells (11, 29a). Conversely, the EGFR/erbB-2 TK1 molecule was a poor mitogenic signal transducer in this hematopoietic cell line, behaving much like gp185^{erbB-2} (11, 29a).

A further genetic analysis of the EGFR TK1 domain revealed that a deletion spanning residues 660 to 667 im-

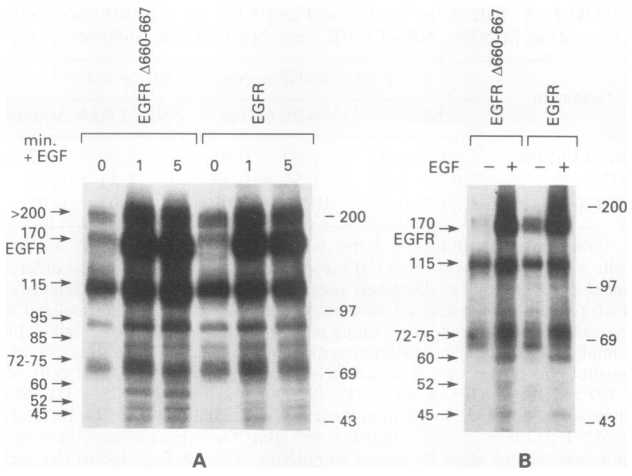

FIG. 10. Tyrosine phosphorylation of cellular proteins by EGFR and EGFR Δ660-667. The NR6-EGFR and NR6-EGFR Δ660-667 cell lines, described in the legend to Fig. 9, and expressing comparable levels of receptor (about 1.0×10^5 receptors per cell, as estimated by ^{125}I-EGF-binding experiments) were used. Cells were either mock treated (− lanes) or treated with EGF (16 nM) at 37°C (+ lanes). (A) Cells were serum-starved for 16 h and then metabolically labeled in the presence of 0.5 mCi of $^{32}P_i$ for 4 h at 37°C, followed by EGF stimulation for 1 or 5 min. Equal amounts of trichloroacetic acid-precipitable cpm were immunoprecipitated with excess anti-PTyr antibodies, and the immunoprecipitates were analyzed by SDS-PAGE on a discontinuous acrylamide gradient gel (top 7.5%, bottom 12.5%). (B) Cells were serum-starved for 16 h and then treated with EGF for 5 min or mock treated. Total cellular proteins (1.0 mg) were immunoprecipitated with excess anti-PTyr antibodies and then analyzed by immunoblotting with anti-PTyr antibodies. Molecular mass markers are indicated in kilodaltons. Arrows point at the PTyr-containing proteins. Results are typical and representative of two independent experiments.

paired transduction of the EGFR mitogenic signal. When the Δ660-667 mutant was expressed at physiological levels in NR6 fibroblasts, we observed both an increase in the EGF ED_{50} and a reduction of the maximal biological response in comparison to NR6-EGFR cells. Loss of affinity for EGF or reduction of the intrinsic catalytic properties of the mutant receptor were excluded as possible causes for its impaired ability to deliver a mitogenic signal. We therefore propose that the Δ660-667 mutation affects the ability of the EGFR kinase to recognize one or possibly more of its cellular substrates. A partial rescue of the Δ660-667 mutation was observed by increased receptor expression. This finding could be explained by the fact that receptor overexpression might either compensate for a reduced affinity of EGFR Δ660-667 for some cellular substrate(s) or allow increased recruitment of substrates whose phosphorylation is not affected by the Δ660-667 mutation.

The effect of the Δ660-667 mutation seems to be quite specific in that other mutations in this region failed to induce the same phenotype. In particular, a Glu-Arg to Asp-Val mutation of residues 661 and 662 did not alter the biochemical and biological properties of the EGFR. On the other hand, the Δ670-674 deletion and the Ser-Gly-Glu → Met-Val-Asn mutation at residues 671 to 673 dramatically impaired the intrinsic catalytic properties of the EGFR kinase. The latter two mutations are located about 25 residues NH_2 terminal to the Gly-X-Gly-X-X-Gly consensus sequence involved in ATP binding (16). It is possible that folding of the molecule in this region juxtaposes structures involved in substrate recognition with those important for the phosphotransferase reaction. By such a model, the 660 to 667 region could therefore play a key role in substrate recognition, whereas the residues COOH terminal to this sequence might be important for the proper folding of the catalytic site.

In this regard, it is interesting that sequence comparison between EGFR and *erbB-2*, in the region corresponding to the Δ660-667 deletion, revealed only one amino acid change of a nonconservative nature, consisting in a Thr for Arg substitution at position 662 of the EGFR (position 694 of *erbB-2*). If this change were important in determining the signalling specificity of the two receptors, one should expect increased mitogenic signalling by a mutant EGFR bearing the Arg-662 to Thr substitution. We are presently engineering such an EGFR-Thr-662 mutant to test its mitogenic activity; we are also attempting the generation of chimeras between the juxtamembrane regions of different tyrosine kinase receptors.

The 660 to 667 sequence is in the proximity of Thr-669 and Ser-671, which have been mapped as sites of phosphorylation of the EGFR (4, 17). We do not know whether the Δ660-667 mutation affects phosphorylation of these residues. However, substitutions at positions 669 and 671 do not appear to have any impact on EGFR mitogenic activity (4). Thus, it is unlikely that altered phosphorylation of these residues may account for the biological effects of the Δ660-667 mutation. The 660 to 667 sequence is also in the proximity of Thr-654, which is a target of protein kinase C phosphorylation (7, 18). Site-directed mutagenesis at Thr-654 has shown that phosphorylation of this residue downregulates EGFR signalling (6, 23). According to Davis (6), this is likely to be due to a reduction of the EGFR intrinsic kinase activity, whereas Livneh et al. (23) have proposed that some allosteric change induced by Thr-654 phosphorylation impairs EGFR signal transduction independently from the protein kinase C-mediated reduction of the EGFR kinase activity. These two mechanisms may not be mutually exclusive. Therefore, phosphorylation of Thr-654 might reduce EGFR kinase activity and also induce an allosteric change whose functional consequence could be similar to that of the Δ660-667 mutation, that is, impaired substrate recognition.

Our data are consistent with those of White et al. (42), who described a Tyr → Phe mutation at position 960 in the human insulin receptor (hIR) which greatly reduced hIR biologic activity without affecting its intrinsic catalytic function. In the comparison of the hIR and EGFR predicted sequences, hIR Tyr-960 falls in the region of the EGFR which is affected by the Δ660-667 mutation. Therefore, mutations affecting analogous regions of two different tyrosine kinase receptors elicit similar biological effects.

That the juxtamembrane region of the EGFR may be involved in specific substrate recognition is further supported by a recent study in which Cochet et al. showed that residues spanning positions 644 through 666 in the human EGFR play a crucial role in directing physical interactions between EGFR and phosphoinositide kinases (3). It will be of interest to analyze whether the Δ660-667 mutation affects these interactions and, if so, whether this has any relevance in EGF-dependent mitogenic signalling.

The identity of the cellular proteins which are phosphorylated on tyrosine residues upon EGF stimulation remains elusive. Recently, however, PLC-γ and the $p21^{ras}$ GTPase-activating protein (GAP) have been shown to be substrates of the EGFR (see reference 37 and references therein). We therefore tried to determine whether the Δ660-667 mutation

affects the ability of the EGFR to phosphorylate these two polypeptides. By using transfectants expressing about 10^5 wild-type EGFRs per cell, we have not been able to detect EGF-stimulated GAP phosphorylation on tyrosine residues under conditions in which tyrosine-phosphorylated GAP was easily detected in PDGF-treated cells (data not shown). This result is consistent with our previous work showing that the stoichiometry of GAP phosphorylation by the EGFR is quite low (14). In addition, we did not detect substantial differences in the ability of the Δ660-667 mutant to phosphorylate PLC-γ or to induce PIP_2 breakdown compared with wild-type EGFR. Therefore, this pathway does not seem to be involved in the impaired mitogenic response elicited by the Δ660-667 mutant.

Our initial attempts at identifying a cellular protein(s) whose phosphorylation on tyrosine residues is adversely affected by the Δ660-667 mutation were not successful. It is likely that phosphorylation of key substrates for mitogenesis is tightly controlled and therefore not readily appreciable in cells expressing normal levels of EGFRs. We are currently developing cell lines with higher receptor content as well as high-resolution methods for more detailed chromatographic analysis of tyrosine-phosphorylated proteins in EGF-stimulated NR6-EGFR Δ660-667 cells. Such studies may lead to the identification of key substrates whose reduced tyrosine phosphorylation accounts for the impaired mitogenic ability of the Δ660-667 mutant.

ACKNOWLEDGMENTS

We are indebted to S. A. Aaronson for continuous encouragement and helpful discussions and for critically reviewing the manuscript. We also thank S. G. Rhee for providing the monoclonal antibodies directed against PLC-γ, E. Appella and K. Sakaguchi for the synthesis and purification of the peptide substrate used in the in vitro kinase assays, and S. Tronick for his advice in computer analysis. We thank N. Duvall for technical assistance and N. Lichtenberg for her delightful patience in typing the manuscript. O.S. wishes to dedicate this study to M.G. and to the whitewater rivers of America.

M.F.W. is a scholar of the Pew Foundation, Philadelphia. F.F. is the recipient of an A.I.R.C. fellowship (Associazione Italiana per la Ricerca sul Cancro). This work was supported in part by grant DK 38712 to M.F.W.

REFERENCES

1. **Carpenter, G.** 1987. Receptors for epidermal growth factor and other polypeptide mitogens. Annu. Rev. Biochem. **56**:881–914.
2. **Chen, W. S., C. S. Lazar, K. A. Lund, J. B. Welsh, C.-P. Chang, G. M. Walton, C. J. Der, H. S. Wiley, G. N. Gill, and M. G. Rosenfeld.** 1989. Functional independence of the epidermal growth factor receptor from a domain required for ligand-induced internalization and calcium regulation. Cell **59**:33–43.
3. **Cochet, C., O. Filhol, B. Payrastre, T. Hunter, and G. N. Gill.** 1991. Interaction between the epidermal growth factor receptor and phosphoinositide kinases. J. Biol. Chem. **266**:637–644.
4. **Countaway, J. L., P. McQuilnick, N. Girones, and R. J. Davis.** 1990. Multisite phosphorylation of the epidermal growth factor receptor. Use of site-directed mutagenesis to examine the role of serine/threonine phosphorylation. J. Biol. Chem. **265**:3407–3416.
5. **Coussens, L., T. L. Yang-Feng, Y. C. Liao, E. Chen, A. Gray, J. McGrath, P. H. Seeburg, T. A. Libermann, J. Schlessinger, U. Francke, A. Levinson, and A. Ullrich.** 1985. Tyrosine kinase receptor with extensive homology to EGF receptor shares chromosomal location with *neu* oncogene. Science **230**:1132–1139.
6. **Davis, R. J.** 1988. Independent mechanisms account for the regulation by protein kinase-C of the EGF-receptor affinity and tyrosine-protein kinase activity. J. Biol. Chem. **263**:9462–9469.
7. **Davis, R. J., and M. P. Czech.** 1985. Tumor-promoting phorbol diesters cause the phosphorylation of epidermal growth factor receptors in normal human fibroblasts at threonine-654. Proc. Natl. Acad. Sci. USA **82**:1974–1978.
8. **Di Fiore, P. P., J. H. Pierce, T. P. Fleming, R. Hazan, A. Ullrich, C. R. King, J. Schlessinger, and S. A. Aaronson.** 1987. Overexpression of the human EGF receptor confers an EGF-dependent transformed phenotype to NIH 3T3 cells. Cell **51**:1063–1070.
9. **Di Fiore, P. P., J. H. Pierce, M. H. Kraus, O. Segatto, C. R. King, and S. A. Aaronson.** 1987. *erbB*-2 is a potent oncogene when overexpressed in NIH/3T3 cells. Science **237**:178–182.
10. **Di Fiore, P. P., O. Segatto, F. Lonardo, F. Fazioli, J. H. Pierce, and S. A. Aaronson.** 1990. The carboxy-terminal domains of *erbB-2* and epidermal growth factor receptor exert different regulatory effects on intrinsic receptor tyrosine kinase function and transforming activity. Mol. Cell. Biol. **10**:2749–2756.
11. **Di Fiore, P. P., O. Segatto, W. G. Taylor, S. A. Aaronson, and J. H. Pierce.** 1990. EGF receptor and *erbB*-2 tyrosine kinase domains confer cell specificity for mitogenic signaling. Science **248**:79–83.
12. **Downing, J. R., B. L. Margolis, Z. Zilberstein, R. A. Ashmun, A. Ullrich, C. J. Sherr, and J. Schlessinger.** 1989. Phospholipase C-γ, a substrate for PDGF receptor kinase, is not phosphorylated on tyrosine residues during the mitogenic response to CSF-1. EMBO J. **8**:3345–3350.
13. **Downward, J., P. Parker, and M. D. Waterfield.** 1984. Autophosphorylation sites on the epidermal growth factor receptors. Nature (London) **311**:483–485.
14. **Fazioli, F., U.-H. Kim, S. G. Rhee, C. J. Molloy, O. Segatto, and P. P. Di Fiore.** 1991. The *erbB-2* mitogenic signalling pathway: tyrosine phosphorylation of phospholipase C-γ and GTPase-activating protein does not correlate with *erbB-2* mitogenic potency. Mol. Cell. Biol. **11**:2040–2048.
15. **Graham, F. L., and A. J. Van der Eb.** 1973. A new technique for the assay of infectivity of human adenovirus 5 DNA. Virology **52**:456–467.
16. **Hanks, S. K., A. M. Quinn, and T. Hunter.** 1988. The protein kinase family: conserved features and deduced phylogeny of the catalytic domains. Science **241**:42–52.
17. **Heisermann, G. J., and G. N. Gill.** 1988. Epidermal growth factor receptor threonine and serine residues phosphorylated in vivo. J. Biol. Chem. **263**:13152–13158.
18. **Hunter, T., N. Ling, and J. A. Cooper.** 1984. Protein kinase C phosphorylation of the EGF receptor at a threonine residue close to the cytoplasmic face of the membrane. Nature (London) **311**:480–483.
19. **Jainchill, J. L., S. A. Aaronson, and G. J. Todaro.** 1969. Murine sarcoma and leukemia viruses: assay using clonal lines of contact-inhibited mouse cells. J. Virol. **4**:549–553.
20. **Kaplan, D. R., D. K. Morrison, G. Wong, F. McCormick, and L. T. Williams.** 1990. PDGF beta-receptor stimulates tyrosine phosphorylation of GAP and association of GAP with a signaling complex. Cell **61**:125–133.
21. **Kazlauskas, A., C. Ellis, T. Pawson, and J. A. Cooper.** 1990. Binding of GAP to activated PDGF receptor. Science **247**:1578–1581.
22. **Kunkel, T. A.** 1985. Rapid and efficient site-specific mutagenesis without phenotypic selection. Proc. Natl. Acad. Sci. USA **82**:488–492.
23. **Livneh, E., T. Dull, R. Prywes, A. Ullrich, and J. Schlessinger.** 1988. Release of phorbol ester-induced mitogenic block by mutation at Thr-654 of epidermal growth factor receptor. Mol. Cell. Biol. **8**:2302–2308.
24. **Margolis, B., S. G. Rhee, S. Felder, M. Mervice, R. Lyall, A. Levitzki, A. Ullrich, A. Zilberstein, and J. Schlessinger.** 1989. EGF induces phosphorylation of phospholipase C-II: a potential mechanism for EGF receptor signaling. Cell **57**:1101–1107.
25. **Meisenhelder, J., P.-G. Suh, S. G. Rhee, and T. Hunter.** 1989. Phospholipase C-γ is a substrate for the PDGF and EGF receptor protein-tyrosine kinase *in vivo* and *in vitro*. Cell **57**:1109–1122.
26. **Molloy, C. J., D. P. Bottaro, T. P. Fleming, M. S. Marshall, J. B. Gibbs, and S. A. Aaronson.** 1989. PDGF induction of tyrosine

phosphorylation of GTPase activating protein. Nature (London) **342**:711–714.

27. **Morrison, D. K., D. R. Kaplan, J. A. Escobedo, U. R. Rapp, T. M. Roberts, and L. T. Williams.** 1989. Direct activation of the serine/threonine kinase activity of Raf-1 through tyrosine phosphorylation by the PDGF β-receptor. Cell **58**:649–657.
28. **Mulligan, R. C., and P. Berg.** 1981. Selection for animal cells that express the *Escherichia coli* gene coding for xanthine-guanine phosphoribosyltransferase. Proc. Natl. Acad. Sci. USA **78**:2072–2076.
29. **Pang, D. T., B. R. Sharma, and J. A. Shafer.** 1985. Purification of the catalytically active phosphorylated form of insulin receptor kinase by affinity chromatography with *O*-phosphotyrosyl-binding antibodies. Arch. Biochem. Biophys. **242**:176–186.

29a. **Pierce, J. H., and P. P. Di Fiore.** Unpublished data.

30. **Pierce, J. H., M. Ruggiero, T. P. Fleming, P. P. Di Fiore, J. S. Greenberger, L. Varticovski, J. Schlessinger, G. Rovera, and S. A. Aaronson.** 1988. Signal transduction through the EGF receptor transfected in IL-3-dependent hematopoietic cells. Science **239**:628–631.
31. **Pruss, R. M., and H. R. Herschmann.** 1977. Variants of 3T3 cells lacking mitogenic response to epidermal growth factor. Proc. Natl. Acad. Sci. USA **74**:3918–3921.
32. **Segatto, O., C. R. King, J. H. Pierce, P. P. Di Fiore, and S. A. Aaronson.** 1988. Different structural alterations upregulate in vitro tyrosine kinase activity and transforming potency of the *erbB-2* gene. Mol. Cell. Biol. **8**:5570–5574.
33. **Segatto, O., F. Lonardo, J. H. Pierce, D. P. Bottaro, and P. P. Di Fiore.** 1990. The role of autophosphorylation in modulation of *erb*B-2 transforming function. New Biol. **2**:187–195.
34. **Stern, D. F., M. P. Kamps, and H. Cao.** 1988. Oncogenic activation of $p185^{neu[00ae]MDNM[00af]}$ stimulates tyrosine phosphorylation in vivo. Mol. Cell. Biol. **8**:3969–3973.
35. **Suh, P.-G., S. H. Ryu, W. C. Choi, K. Y. Lee, and S. G. Rhee.** 1988. Monoclonal antibodies to three phospholipase C isozymes from bovine brain. J. Biol. Chem. **263**:14497–14504.
36. **Ullrich, A., L. Coussens, J. S. Hayflick, T. J. Dull, A. Gray, A. W. Tam, J. Lee, Y. Yarden, T. A. Libermann, J. Schlessinger, J. Downward, E. L. V. Mayes, N. Whittle, M. D. Waterfield, and P. H. Seeburg.** 1984. Human epidermal growth factor receptor cDNA sequence and aberrant expression of the amplified gene in A431 epidermoid carcinoma cells. Nature (London) **309**:418–425.
37. **Ullrich, A., and J. Schlessinger.** 1990. Signal transduction by receptors with tyrosine kinase activity. Cell **61**:203–212.
38. **Varticovski, L., B. Druker, D. Morrison, L. Cantley, and T. Roberts.** 1989. The colony stimulating factor-1 receptor associates with and activates phosphatidylinositol-3 kinase. Nature (London) **342**:699–702.
39. **Wahl, M. I., N. E. Olashaw, S. Nishibe, S. G. Rhee, W. J. Pledger, and G. Carpenter.** 1989. Platelet-derived growth factor induces rapid and sustained tyrosine phosphorylation of phospholipase C-γ in quiescent BALB/c 3T3 cells. Mol. Cell. Biol. **9**:2934–2943.
40. **Wahl, M. I., S. Nishibe, P.-G. Suh, S. G. Rhee, and G. Carpenter.** 1989. Epidermal growth factor stimulates tyrosine phosphorylation of phospholipase C-II independently of receptor internalization and extracellular calcium. Proc. Natl. Acad. Sci. USA **86**:1568–1572.
41. **Walton, G. M., W. S. Chen, M. G. Rosenfeld, and G. N. Gill.** 1990. Analysis of the carboxyl-terminus of the epidermal growth factor receptor reveals self-phosphorylation at tyrosine 992 and enhanced *in vivo* tyrosine phosphorylation of cell substrates. J. Biol. Chem. **265**:1750–1754.
42. **White, M. F., J. N. Livingston, J. M. Backer, V. Lauris, T. J. Dull, A. Ullrich, and C. R. Kahn.** 1988. Mutation of the insulin receptor at tyrosine 960 inhibits signal transmission but does not affect its tyrosine kinase activity. Cell **54**:641–649.
43. **Wigler, M., S. Silverstein, L. S. Lee, A. Pellicer, Y.-C. Cheng, and R. Axel.** 1977. Transfer of purified herpes virus thymidine kinase gene to cultured mouse cells. Cell **11**:223–232.
44. **Williams, L. T.** 1989. Signal transduction by the platelet-derived growth factor receptor. Science **243**:1564–1570.
45. **Yarden, Y., and A. Ullrich.** 1988. Growth factor receptor tyrosine kinases. Annu. Rev. Biochem. **57**:443–478.